Matter and Radiation at Extremes | RESEARCH ARTICLE | pubs.aip.org/aip/mre

A fresh class of superconducting and hard pentaborides

Cite as: Matter Radiat. Extremes 8, 058404 (2023); doi: 10.1063/5.0157250
Submitted: 6 May 2023 • Accepted: 10 August 2023 •
Published Online: 6 September 2023

Hui Xie,[1,a)] Hong Wang,[1] Fang Qin,[1] Wei Han,[1] Suxin Wang,[1] Youchun Wang,[2,a)] Fubo Tian,[3] and Defang Duan[3,a)]

AFFILIATIONS

[1] College of Physics and Electronic Engineering, Hebei Normal University for Nationalities, Chengde 067000, China
[2] College of Physics and Electronic Engineering, Linyi University, Linyi 276000, China
[3] College of Physics, Jilin University, Changchun 130012, China

Note: Paper published as part of the Special Topic on High Pressure Science 2023.
[a)] **Authors to whom correspondence should be addressed:** huixie@hbun.edu.cn; wangyouchun@lyu.edu.cn; and duandf@jlu.edu.cn

ABSTRACT

On the basis of the current theoretical understanding of boron-based hard superconductors under ambient conditions, numerous studies have been conducted with the aim of developing superconducting materials with favorable mechanical properties using boron-rich compounds. In this paper, first-principles calculations reveal the existence of an unprecedented family of tetragonal pentaborides MB_5 (M = Na, K, Rb, Ca, Sr, Ba, Sc, and Y), comprising B_{20} cages and centered metal atoms acting as stabilizers and electron donors to the boron sublattice. These compounds exhibit both superconductivity and high hardness, with the maximum superconducting transition temperature T_c of 18.6 K being achieved in RbB_5 and the peak Vickers hardness H_v of 35.1 GPa being achieved in KB_5 at 1 atm. The combination of these properties is particularly evident in KB_5, RbB_5, and BaB_5, with T_c values of ~14.7, 18.6, and 16.3 K and H_v values of ~35.1, 32.4, and 33.8 GPa, respectively. The results presented here reveal that pentaborides can provide a framework for exploring and designing novel superconducting materials with favorable hardness at achievable pressures and even under ambient conditions.

I. INTRODUCTION

Superconducting and superhard substances have been at the forefront of fundamental research and industrial applications. High-pressure syntheses and theoretical predictions[1–12] have been performed to investigate the superconductivity of various materials such as copper/iron-based superconductors,[13,14] as well as conventional Bardeen–Cooper–Schrieffer (BCS) superconductors. In view of the tremendous advances that have been achieved in enhancing the transition temperatures of conventional phonon-mediated superconductors, especially of highly compressed hydrides, it is natural to investigate superconductivity in other lightweight materials. This class of compounds containing light elements are excellent candidates for superhard materials.[15]

Borides have attracted considerable attention in research into superconductivity and hardness because of the diversity of their crystal chemistry.[16] In early work, Japanese scientists reported superconductivity of MgB_2 at 39 K under ambient pressure,[1] fueling enthusiasm for a search for high-temperature superconductivity in the compressed borides.[17–24] Polycrystalline MgB_2 synthesized by high-pressure sintering is a superhard material[25] with Vickers hardness H_v up to 4109.5 kg/cm^2. Thus, the idea of developing novel superhard materials using borides and with desired characteristics has gained traction.[18,24,26–28] B_6C is a superconducting and superhard material, with a transition temperature T_c of ~12.5 K and an H_v of ~48 GPa at ambient pressure.[29] Theoretical studies[30] have revealed that α-BeB_6 is superconducting and superhard with T_c of 9 K and H_v of 46 GPa. At high pressure, the predicted T_c and H_v of β-BeB_6 are up to 24 K and 31 GPa, respectively. Du *et al.*[23] performed electron–phonon coupling (EPC) and mechanical calculations demonstrating that ScB_6 phases have estimated transition temperatures and hardnesses of ~2.2–5.8 K and 16.2–27.3 GPa under extreme conditions. Lately, Liu's group have designed a novel class of clathrate-like superconductors, MB_7, with superior hardness, among which the T_c and H_v of KB_7 were estimated to be 26.2 K and 22.5 GPa at 1 atm. On the basis of previous results,[16] borides

tend to be hard or superhard materials, with these properties being derived from the covalent boron sublattice. However, although there have been extensive attempts to find high-temperature boron-based superconductors, theoretical and experimental success is yet to be realized. The lower T_c values of two- or three-dimensional borides compared with those of compressed hydrides has motivated us to perform a systematic investigation in this exciting field with a view to finding a new type of superconducting structure with high hardness.

Yttrium borides form various stoichiometries with excellent thermoelastic, electronic, and mechanical properties, which can be systematically applied in various industries.[16,27,31] YB_2, YB_4, YB_6, YB_{12}, and YB_{66} are stable under ambient conditions, with H_v around 25.3–40.9 GPa.[16,32,33] Furthermore, the T_c values of YB_6 and YB_{12} are 1.8–12.8 and 4.7 K.[17,34,35] We have performed extensive random structure searches for stable or metastable YB_{2-12} compounds under high pressures and have discovered a novel superconductor, yttrium pentaboride, with a T_c of 12.3 K. In YB_5, B atoms are strongly covalently bonded to each other within B_{20} cages, with Y atoms occupying the centers of these cages and acting as electron donors. A new group of pentaborides, MB_5 (M = Na, K, Rb, Ca, Sr, Ba, and Sc), isomorphic to the predicted YB_5, have also been estimated to exhibit high superconducting transition temperatures (T_{cmax} = 18.6 K) and hardness (H_{vmax} = 35.1 GPa). This study lays the foundation for exploring new classes of hard boron-based superconductors and provides valuable guidance for further experimental syntheses.

II. COMPUTATIONAL DETAILS

High-pressure structural predictions of YB_{2-12} were performed as implemented in the AIRSS code[36] at pressures of 1 atm, 50 GPa, and 100 GPa,[36] generating ~10 000 structures randomly. The CASTEP code,[37] on-the-fly pseudopotentials, the Perdew–Burke–Ernzerhof (PBE) generalized gradient approximation (GGA)[38] exchange-correlation functional, and $4s^2 4p^6 4d^1 5s^2$ (Y) and $2s^2 2p^1$ (B) valence electrons were used during the random structure searches and geometrical optimizations. The kinetic energy cutoff and k-spacing were fixed appropriately at 800 eV and $2\pi \times 0.03$ Å^{-1} in structure optimizations. Electronic characters were calculated using the Vienna *Ab initio* Simulation Package (VASP)[39] and the all-electron projector-augmented wave method (PAW) pseudopotentials. The *ab initio* molecular dynamics (AIMD) simulations were carried out in the framework of the Nosé–Hoover method.[40] The phonon dispersions were calculated with the supercell approach[41] as used in the phonopy code.[42] Electron–phonon coupling was computed by the Quantum ESPRESSO package,[43] using a norm-conserving scheme with an energy cutoff of 80 Ry, a k-mesh of 24 × 24 × 24 and a q-mesh of 4 × 4 × 4. The superconducting transition temperatures of MB_5 were approximated with the Allen–Dynes modified McMillan equation[44]

$$T_c = \frac{\omega_{\log}}{1.2} \exp\left[-\frac{1.04(1+\lambda)}{\lambda - \mu^*(1+0.62\lambda)}\right], \quad (1)$$

where μ^* is the Coulomb pseudopotential, and $\omega_{\log}$ is the logarithmic average frequency and is defined as follows:

$$\omega_{\log} = \exp\left[\frac{2}{\lambda}\int \frac{d\omega}{\omega}\alpha^2 F(\omega)\ln\omega\right]. \quad (2)$$

The EPC constant λ can be calculated as follows:

$$\lambda = 2\int \frac{\alpha^2 F(\omega)}{\omega} d\omega. \quad (3)$$

The elastic constants were computed using the VASP code, applying the strain–stress method. The mechanical moduli and H_v were derived from the elastic constants using the Voigt–Reuss–Hill approximation[45] and the model proposed by Chen *et al.*[46]

III. RESULTS AND DISCUSSION

We investigated structures under ambient pressure and reproduced the previously known phases of YB_2, YB_4, YB_6, and YB_{12}, confirming the reliability of our predictions. The lattice parameters of the optimized structures are consistent with known experimental findings,[16] as presented in Table S1 (supplementary material). The formation enthalpies ΔH of the predicted YB_{2-12} stoichiometries were calculated with respect to the pure elements at 1 atm, 50 GPa, and 100 GPa [see Fig. 1(a)], from which the convex hull was constructed. The known $R\bar{3}m$, *Pnnm*, and *Cmca* structures for boron[47] and the hcp, dhcp, and $P6_222$ structures for yttrium[48] were adopted in their corresponding stable pressure. The results revealed that YB_2, YB_4, and YB_{12}, as expected, are stable at atmospheric pressure. Cubic YB_6 is metastable at ~31 meV/atom above the convex hull, which does not show that our calculations are unreliable or that the material cannot be synthesized experimentally. The fact that the compound is in a metastable state means that the predicted effect can be observed in actual high-temperature experiments.[49] At 50 GPa, the stable configurations remain the same, and $I4/mmm$–YB_6 emerges on the convex hull. Hexagonal YB_2 emerges as the most stable compound in the studied pressure ranges all along. With the pressure increased to 100 GPa, the stable structure of YB_4 changes to $C2/m$. Meanwhile, YB_{12} deviates from the tieline and decomposes into YB_6 and B, whereas another unreported boron-rich composition $P4/mmm$–YB_5 is close to the convex hull (~35 meV). The phonon bands of these structures manifest their dynamic stability, since the no imaginary frequency appears in the Brillouin zone (see Fig. S1, supplementary material). In the following discussion, the novel YB_5 structure is the main focus because it has relative high symmetry and is recoverable to ambient pressure.

Yttrium pentaboride adopts a tetragonal $P4/mmm$ space group [see Fig. 1(b)], where B atoms occupy 4n and 1d positions bonding to each other within the B_{20} cage [see Fig. 1(c)], and Y atoms lies at the crystallographic 1b position occupying the centers of the B_{20} cages. This structure is similar to that of cubic YB_6, in which B atoms constitute a boron octahedral network. The straight chains of boron octahedrons are arranged in a three-dimensional frame. This three-dimensional clathrate-like B_{20} structure with metal atoms filling the B cages is also found in NaB_5, KB_5, RbB_5, CaB_5, SrB_5, BaB_5, and ScB_5 through isostructural metal atom replacement at 100 GPa, with each material showing thermal stability (see Fig. S2, supplementary material). Phonon calculations reveal their dynamic stability at ambient pressure (Fig. S3, supplementary material). The electron localization function (ELF)[50] was calculated to map the electron pair probability and understand interatomic interactions. No charge localization appears between boron and metal atoms, providing evidence for M–B ionic bonding (see Fig S4, supplementary

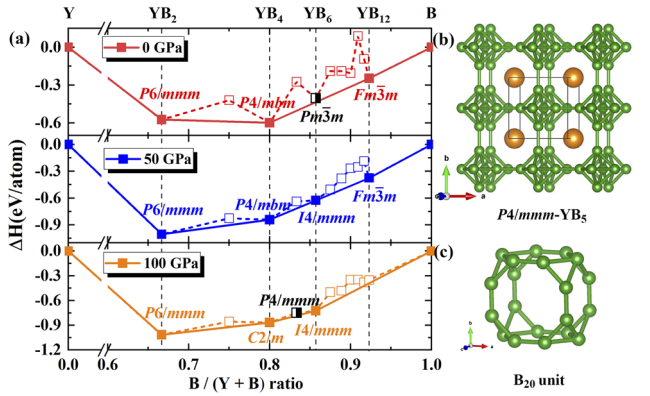

FIG. 1. (a) Enthalpies of formation of predicted YB_{2-12} as functions of B concentration at 1 atm, 50 GPa, and 100 GPa. Open, half-filled, and filled symbols represent unstable, metastable, and stable stoichiometries, respectively, relative to the elementary substance. (b) Crystal structures of *P*4/*mmm*–YB_5. (c) The B_{20} unit. Y and B atoms are presented as golden and green spheres. The cutoff distance between B–B bonds is 2.0 Å.

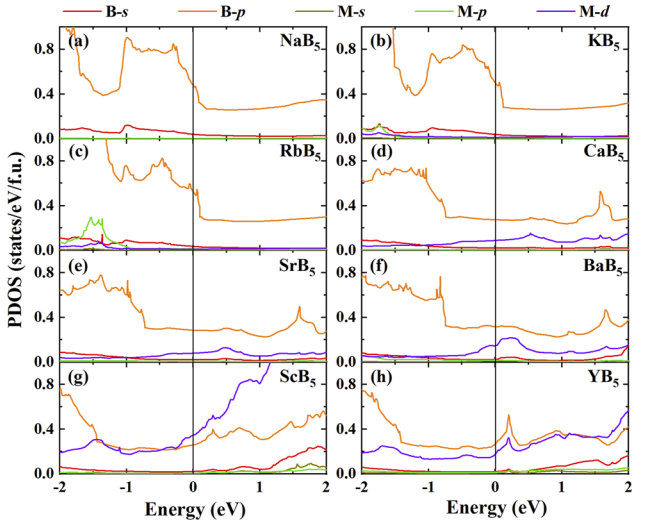

FIG. 2. Calculated electronic projected DOS for *P*4/*mmm*-MB_5 (M = Li, Na, K, Rb, Ca, Sr, Ba, Sc, and Y) at 1 atm. The black line where the energy is equal to zero is the Fermi level.

material). Bader charge analysis was also performed to calculate the transferred charge between atoms (see Table S2, supplementary material). The metal atoms serve as electron donors to the boron sublattice, which is also supported by the ELF results. The ELF values between B–B bonds in the three-dimensional frameworks of the metal pentaborides are larger than 0.7, implying the formation of covalent bonds. Among them, the ELF between two adjacent boron octahedrons is approximately equal to or even greater than 0.9, which is greater than that between B5 (the B atom shared between adjacent boron octahedrons) and its neighboring atoms, which has a range of 0.7–0.8. The integrated crystal orbital Hamilton population (ICOHP) of adjacent B–B pairs with bond lengths of 1.6–2.0 Å was calculated using the LOBSTER package[51] to further confirm their covalent characteristics. The negative ICOHP values of B–B pairs in the above structures indicate B–B covalent interactions. As displayed in Fig. S5 (supplementary material), the ICOHP values of B1–B2 (B3–B4) pairs in MB_5 are in the range of −7.8 to −5.4 eV/pair, which indicates strong covalent bonding. The B1–B3 (B1–B4, B2–B3 or B2–B4) bonds are fairly strong, with ICOHP values of −5.4 to −2.7 eV/pair, stronger than or approximately equal to that of B5–B1 (B5–B2, B5–B3, or B5–B4, −3.6 to −2.9 eV/pair) bonds. The ICOHP values are consistent with the ELF results.

A high electronic density of states (DOS) is a guideline for successful searches for new superconducting materials, and therefore the projected DOS of MB_5 at atmospheric pressure was calculated. Note that all the studied compounds are metallic, as presented in Fig. 2. In the alkali metal (AMB_5) and the light alkaline earth metal ($AEMB_5$) pentaborides, the greatest contribution to the DOS close to the Fermi energy E_f is provided by the B-*p* orbital [see Figs. 2(a)–2(e)], although the M-*d* orbital at E_f does play a non-negligible role in their metallicity. (It should also be mentioned that the electronic DOS of alkali metal pentaborides has a van Hove singularity near E_f, implying fairly strong electron–phonon interactions associated with boron phonon modes.) By contrast, in BaB_5 and the rare-earth borides ScB_5 and YB_5, the DOS values are dominated by both the M-*d* and B-*p* orbitals [see Figs. 2(f)–2(h)]. In addition, ScB_5 exhibits a particularly high DOS at the Fermi level (see Fig. S6, supplementary material).

The conclusions regarding the electronic DOS are further confirmed by the results for electron–phonon coupling (EPC). The calculated Eliashberg spectral function $\alpha^2F(\omega)$ and the EPC parameter $\lambda(\omega)$ at ambient pressure are shown in Fig. 3. Clearly, EPC in the AMB_5, BaB_5, and ScB_5 is much more prominent than in the light $AEMB_5$ and YB_5. The calculated EPC values, logarithmic average phonon frequency ω_{log}, electronic DOS near the Fermi energy $N(E_f)$, and superconducting transition temperatures T_c are presented in Table I. The estimated λ values of NaB_5 and KB_5 are 0.73 and 0.64, respectively, and the corresponding values of T_c are 17.5 and 14.7 K when the Coulomb potential parameter μ^* equals 0.1. According to the phonon DOS (PHDOS) illustrated in Figs. 3(a) and 3(b), vibrations can be separated into low-frequency and high-frequency regions. The low-frequency modes (<8 THz) contribute 52% and 35%, respectively, comprising a mixture of vibrations from M (M = Na and K) and B atoms. EPC calculation for RbB_5 gives a relatively large λ of 0.78, which is primarily associated with the high-lying frequencies (>6 THz) of boron (~63%) [see Fig. 3(c)], yielding an estimated T_c of 18.6 K. The estimated T_c values for CaB_5 and SrB_5 are 6.6 and 6.8 K, respectively. For the calculated λ of 0.49 and 0.50, as presented in Figs. 3(d) and 3(e), the high-frequency B vibrational modes contribute about 88% and 90%, respectively. The high ω_{log} and $N(E_f)$ values cannot considerably improve T_c, whereas the weak electron–phonon interaction limits the superconductivity of these compounds. In BaB_5, ω_{log} is slightly lower than in the CaB_5 and SrB_5 phases. However, T_c reaches 16.3 K, flowing from the higher λ of 0.73. The contribution of 88% to the total EPC is closely related to the high-frequency vibrations. As can be seen, although ScB_5 has a stronger EPC interaction and higher $N(E_f)$ than the other pentaborides, its ω_{log} is quite low, which is caused by λ and is not

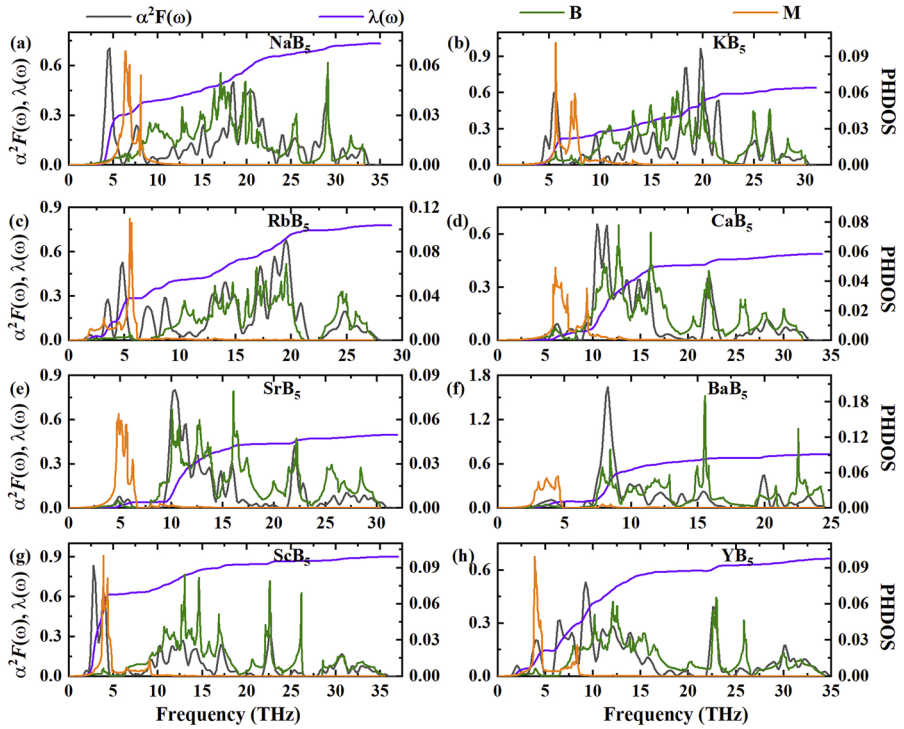

FIG. 3. Eliashberg spectral function $\alpha^2F(\omega)$, EPC parameter $\lambda(\omega)$, and PHDOS of MB_5 at 1 atm.

favorable to T_c. The estimated superconducting transition temperature is ~14.2 K. YB_5 is also predicted to be superconducting, with a T_c of 12.3 K, and corresponding ω_{log} and λ of 403.8 K and 0.66, respectively. We note that the T_c values of borides are not strongly dependent on the contributions of the DOS of boron atoms to the total DOS at the Fermi energy or the electron–phonon interactions of boron to the total λ.

Compared with high-temperature hydrogen-based superconductors, it is obvious that the EPC parameter λ and ω_{log} of the borides are much lower owing to the higher mass of boron. However, only a limited difference is observed in $N(E_f)$, a manifestation of the fact that it is the low values of λ and ω_{log} that lie at the root of the poorer superconductivity of the borides. However, borides can be stabilized at attainable pressures or even ambient pressure, indicating their higher application potential.

To investigate the mechanical characteristics of the MB_5 compounds, we calculated their elastic constants C_{ij} under ambient conditions, from which we derived the bulk modulus B, shear modulus G, Young's modulus Y, Poisson's ratio ν, and Vickers hardness, as presented in Table II. We estimated the hardness of the novel pentaborides to accurately evaluate their incompressibility using Chen's theoretical model[46] as follows:

$$H_v = 2(k^2G)^{0.585} - 3, \quad (4)$$

where k is the ratio of the shear modulus to the bulk modules (Pugh's modulus ratio). It is found that the calculated H_v of the MB_5 compounds is in the range of 7.9–35.1 GPa, with KB_5 showing the highest hardness, which can be attributed to its high values of k and G. Other pentaborides RbB_5, CaB_5, SrB_5, and BaB_5 exhibit superior mechanical properties, with H_v above 30 GPa. Furthermore, charge transfer affects the hardness. From the $\delta(e)$ values of the metal atoms in MB_5 with high hardness (H_v > 30 GPa) presented in Table S2 (supplementary material), one finds that the metal atoms in AMB_5 and $AEMB_5$ transfer approximately (0.6–0.7)e and (1.2–1.4)e, respectively. It seems that this is a reliable new way to identify hard superconducting materials among metastable structures with high symmetry.

TABLE I. Calculated EPC parameter λ, logarithmic average phonon frequency ω_{log}, electronic DOS at the Fermi level $N(E_f)$, and superconducting transition temperature T_c of *P4/mmm*-MB_5, with a Coulomb pseudopotential μ^* = 0.1 at 1 atm.

Boride	λ	ω_{log}	$N(E_f)$ (states Ry^{-1} f.u.$^{-1}$)	T_c (K)
NaB_5	0.73	454.3	4.94	17.5
KB_5	0.64	535.6	5.05	14.7
RbB_5	0.78	420.0	5.07	18.6
CaB_5	0.49	604.7	5.15	6.6
SrB_5	0.50	574.9	5.21	6.8
BaB_5	0.73	420.4	6.07	16.3
ScB_5	0.90	242.1	7.51	14.2
YB_5	0.66	403.8	5.67	12.3

TABLE II. Calculated elastic constants C_{ij} (GPa) and derived bulk modulus B (GPa), shear modulus G (GPa), Young's modulus Y (GPa), Poisson's ratio ν, and hardness H_v (GPa) at ambient pressure. The elastic constants of all the MB_5 compounds satisfy the mechanical stability criterion.[52]

Borides	C_{11}	C_{33}	C_{44}	C_{66}	C_{12}	C_{13}	B	G	Y	ν	H_v
NaB_5	421.2	398.6	74.9	113.6	112.9	8.1	165	117	284	0.21	18.7
KB_5	424.4	331.7	125.4	181	53	30.3	155	155	384	0.13	35.1
RbB_5	340.5	323.7	119.1	177.2	85.5	24.3	141	139	314	0.13	32.4
CaB_5	541.1	415.7	107.8	158.1	51.5	15.8	183	159	370	0.16	30.0
SrB_5	504.7	347.7	116.5	193.7	46.6	33.9	173	162	370	0.14	33.1
BaB_5	399.5	330.1	133.4	207.4	92.2	40.2	162	156	355	0.14	33.8
ScB_5	530.8	433	53.8	100.6	107.3	52.7	211	108	276	0.28	11.1
YB_5	564.2	375.2	59.6	162.5	78.7	49.7	202	123	307	0.25	15.8

IV. CONCLUSIONS

Our extensive structure searches combined with first-principles calculations have revealed the appearance of a metastable clathrate-like B_{20} structure in tetragonal MB_5 (M = Na, K, Rb, Ca, Sr, Ba, Sc, and Y), adopting $P4/mmm$ symmetry. In this structure, metal atoms act as donors to transfer charges to B, and B atoms form a three-dimensional boron octahedral covalent network. Density of states calculations show that the pentaborides are metallic and that the electronic states occupying the Fermi level come mainly from boron atoms. Calculated electron–phonon couplings and elastic constants indicate that the cage-like B_{20} structure can be viewed as a structural model for hard superconductors, with an estimated highest T_c of 18.6 K and a maximum H_v of 35.1 GPa at 1 atm. It is worth mentioning that KB_5, RbB_5 and BaB_5 are superconducting and hard materials, in which the corresponding superconducting critical temperatures are estimated to be around 14.7, 18.6, and 16.3 K and the Vickers hardness to be 35.1, 32.4, and 33.8 GPa, respectively. Our work provides a reference for future experiments and demonstrates that metastable borides hold considerable promise as superconductors with superior hardness at achievable pressures.

SUPPLEMENTARY MATERIAL

See the supplementary material for supplementary figures and tables.

ACKNOWLEDGMENTS

We thank Dr. Yunxian Liu and Dr. Zihao Huo for AIMD calculations and many stimulating discussions. This work was supported by the National Natural Science Foundation of China (Grant Nos. 12104127 and 22131006), the Doctoral Starting Up Foundation of Hebei Normal University for Nationalities (Grant No. DR2020001), the Clean Energy (Carbon Peaking and Carbon Neutrality) Industry Research Institute of Chengde (Grant No. 202205B090), and the Natural Science Foundation of Shandong Province (Grant No. ZR2020QA060). Parts of the calculations were performed at the High Performance Computing Center of Shandong Bailing Cloud Computing Co., Ltd.

AUTHOR DECLARATIONS

Conflict of Interest

The authors have no conflicts to disclose.

Author Contributions

Hui Xie: Conceptualization (equal); Data curation (equal); Investigation (equal); Writing – original draft (equal); Writing – review & editing (equal). **Hong Wang**: Data curation (equal); Formal analysis (equal); Writing – original draft (equal). **Fang Qin**: Investigation (equal). **Wei Han**: Investigation (equal). **Suxin Wang**: Investigation (equal). **Youchun Wang**: Conceptualization (equal); Data curation (equal); Investigation (equal). **Fubo Tian**: Software (equal); Writing – review & editing (equal). **Defang Duan**: Conceptualization (equal); Investigation (equal); Software (equal); Writing – review & editing (equal).

DATA AVAILABILITY

The data that support the findings of this study are available within the article and its supplemental material and from the corresponding authors upon reasonable request.

REFERENCES

[1] J. Nagamatsu, N. Nakagawa, T. Muranaka, Y. Zenitani, and J. Akimitsu, "Superconductivity at 39 K in magnesium diboride," Nature **410**, 63–64 (2001).
[2] D. Duan, X. Huang, F. Tian, D. Li, H. Yu, Y. Liu, Y. Ma, B. Liu, and T. Cui, "Pressure-induced decomposition of solid hydrogen sulfide," Phys. Rev. B **91**, 180502 (2015).
[3] D. Duan, Y. Liu, Y. Ma, Z. Shao, B. Liu, and T. Cui, "Structure and superconductivity of hydrides at high pressures," Natl. Sci. Rev. **4**, 121–135 (2016).
[4] A. P. Drozdov, M. I. Eremets, I. A. Troyan, V. Ksenofontov, and S. I. Shylin, "Conventional superconductivity at 203 kelvin at high pressures in the sulfur hydride system," Nature **525**, 73 (2015).
[5] H. Xie, D. Duan, Z. Shao, H. Song, Y. Wang, X. Xiao, D. Li, F. Tian, B. Liu, and T. Cui, "High-temperature superconductivity in ternary clathrate $YCaH_{12}$ under high pressures," J. Phys.: Condens. Matter **31**, 245404 (2019).
[6] H. Xie, Y. Yao, X. Feng, D. Duan, H. Song, Z. Zhang, S. Jiang, S. A. T. Redfern, V. Z. Kresin, C. J. Pickard, and T. Cui, "Hydrogen pentagraphenelike structure stabilized by hafnium: A high-temperature conventional superconductor," Phys. Rev. Lett. **125**, 217001 (2020).

[7]Z. Zhang, T. Cui, M. J. Hutcheon, A. M. Shipley, H. Song, M. Du, V. Z. Kresin, D. Duan, C. J. Pickard, and Y. Yao, "Design principles for high-temperature superconductors with a hydrogen-based alloy backbone at moderate pressure," Phys. Rev. Lett. **128**, 047001 (2022).
[8]S. Lu, H. Liu, I. I. Naumov, S. Meng, Y. Li, J. S. Tse, B. Yang, and R. J. Hemley, "Superconductivity in dense carbon-based materials," Phys. Rev. B **93**, 104509 (2016).
[9]F. Peng, Y. Sun, C. J. Pickard, R. J. Needs, Q. Wu, and Y. Ma, "Hydrogen clathrate structures in rare earth hydrides at high pressures: Possible route to room-temperature superconductivity," Phys. Rev. Lett. **119**, 107001 (2017).
[10]Z. M. Geballe, H. Liu, A. K. Mishra, M. Ahart, M. Somayazulu, Y. Meng, M. Baldini, and R. J. Hemley, "Synthesis and stability of lanthanum superhydrides," Angew. Chem., Int. Ed. **57**, 688–692 (2018).
[11]A. P. Drozdov, P. P. Kong, V. S. Minkov, S. P. Besedin, M. A. Kuzovnikov, S. Mozaffari, L. Balicas, F. F. Balakirev, D. E. Graf, V. B. Prakapenka, E. Greenberg, D. A. Knyazev, M. Tkacz, and M. I. Eremets, "Superconductivity at 250 K in lanthanum hydride under high pressures," Nature **569**, 528–531 (2019).
[12]M. Somayazulu, M. Ahart, A. K. Mishra, Z. M. Geballe, M. Baldini, Y. Meng, V. V. Struzhkin, and R. J. Hemley, "Evidence for superconductivity above 260 K in lanthanum superhydride at megabar pressures," Phys. Rev. Lett. **122**, 027001 (2019).
[13]M. A. G. Aranda, "Crystal structures of copper-based high-T_c superconductors," Adv. Mater. **6**, 905–921 (1994).
[14]P. Dai, "Antiferromagnetic order and spin dynamics in iron-based superconductors," Rev. Mod. Phys. **87**, 855–896 (2015).
[15]R. B. Kaner, J. J. Gilman, and S. H. Tolbert, "Designing superhard materials," Science **308**, 1268–1269 (2005).
[16]G. Akopov, M. T. Yeung, and R. B. Kaner, "Rediscovering the crystal chemistry of borides," Adv. Mater. **29**, 1604506 (2017).
[17]Y. Xu, L. Zhang, T. Cui, Y. Li, Y. Xie, W. Yu, Y. Ma, and G. Zou, "First-principles study of the lattice dynamics, thermodynamic properties and electron-phonon coupling of YB_6," Phys. Rev. B **76**, 214103 (2007).
[18]M. M. Davari Esfahani, Q. Zhu, H. Dong, A. R. Oganov, S. Wang, M. S. Rakitin, and X. F. Zhou, "Novel magnesium borides and their superconductivity," Phys. Chem. Chem. Phys. **19**, 14486–14494 (2017).
[19]X. Liang, A. Bergara, Y. Xie, L. Wang, R. Sun, Y. Gao, X.-F. Zhou, B. Xu, J. He, D. Yu, G. Gao, and Y. Tian, "Prediction of superconductivity in pressure-induced new silicon boride phases," Phys. Rev. B **101**, 014112 (2020).
[20]Z.-F. Ouyang, X.-W. Yan, and M. Gao, "Electronic structure, phonons, and high-temperature phonon-mediated superconductivity in lithium-intercalated diamond-like boron compounds," Appl. Phys. Express **13**, 083003 (2020).
[21]Y. Liang, M. Xu, S. Lin, X. Yuan, Z. Qu, J. Hao, and Y. Li, "Pressure-induced boron clathrates with ambient-pressure superconductivity," J. Mater. Chem. C **9**, 13782–13788 (2021).
[22]L. Ma, X. Yang, G. Liu, H. Liu, G. Yang, H. Wang, J. Cai, M. Zhou, and H. Wang, "Design and synthesis of clathrate LaB_8 with superconductivity," Phys. Rev. B **104**, 174112 (2021).
[23]J. Du, X. Li, and F. Peng, "Pressure-induced evolution of structures and promising superconductivity of ScB_6," Phys. Chem. Chem. Phys. **24**, 10079–10084 (2022).
[24]S. Han, L. Yu, Y. Liu, B. Zhao, C. Wang, X. Chen, Y. Zhang, R. Yu, and X. Liu, "Clathrate-like alkali and alkaline-earth metal borides: A new family of superconductors with superior hardness," Adv. Funct. Mater. **33**, 2213377 (2023).
[25]H. A. Ma, X. P. Jia, L. X. Chen, P. W. Zhu, G. Z. Ren, W. L. Guo, X. Q. Fu, G. T. Zou, Z. A. Ren, G. C. Che, and Z. X. Zhao, "Superhard MgB_2 bulk material prepared by high-pressure sintering," J. Phys.: Condens. Matter **14**, 11181 (2002).
[26]S. Wei, D. Li, Y. Lv, Z. Liu, F. Tian, D. Duan, B. Liu, and T. Cui, "Strong covalent boron bonding induced extreme hardness of VB_3," J. Alloys Compd. **688**, 1101–1107 (2016).
[27]L. P. Ding, Y. H. Tiandong, P. Shao, Y. Tang, Z. L. Zhao, and H. Lu, "Crystal structures, phase stabilities, electronic properties, and hardness of yttrium borides: New insight from first-principles calculations," J. Phys. Chem. Lett. **12**, 5423–5429 (2021).
[28]K. Zhao, Q. Wang, W. Li, Q. Yang, H. Yu, F. Han, H. Liu, and S. Zhang, "Orthorhombic ScB_3 and hexagonal ScB_6 with high hardness," Phys. Rev. B **105**, 094104 (2022).
[29]K. Xia, M. D. Ma, C. Liu, H. Gao, Q. Chen, J. L. He, J. Sun, H. T. Wang, Y. J. Tian, and D. Y. Xing, "Superhard and superconducting B_6C," Mater. Today Phys. **3**, 76–84 (2017).
[30]L. Wu, B. Wan, H. Liu, H. Gou, Y. Yao, Z. Li, J. Zhang, F. Gao, and H.-k. Mao, "Coexistence of superconductivity and superhardness in beryllium hexaboride driven by inherent multicenter bonding," J. Phys. Chem. Lett. **7**, 4898–4904 (2016).
[31]A. Waśkowska, L. Gerward, J. Staun Olsen, K. Ramesh Babu, G. Vaitheeswaran, V. Kanchana, A. Svane, V. B. Filipov, G. Levchenko, and A. Lyaschenko, "Thermoelastic properties of ScB_2, TiB_2, YB_4 and HoB_4: Experimental and theoretical studies," Acta Mater. **59**, 4886–4894 (2011).
[32]P. K. Liao and K. E. Spear, "The B-Y (boron-yttrium) system," J. Phase Equilib. **16**, 521–524 (1995).
[33]Y. Zhou, H. Xiang, Z. Feng, and Z. Li, "General trends in electronic structure, stability, chemical bonding and mechanical properties of ultrahigh temperature ceramics TMB_2 (TM = transition metal)," J. Mater. Sci. Technol. **31**, 285–294 (2015).
[34]B. T. Matthias, T. H. Geballe, K. Andres, E. Corenzwit, G. W. Hull, and J. P. Maita, "Superconductivity and antiferromagnetism in boron-rich lattices," Science **159**, 530 (1968).
[35]J. Wang, X. Song, X. Shao, B. Gao, Q. Li, and Y. Ma, "High-pressure evolution of unexpected chemical bonding and promising superconducting properties of YB_6," J. Phys. Chem. C **122**, 27820–27828 (2018).
[36]C. J. Pickard and R. J. Needs, "*Ab initio* random structure searching," J. Phys.: Condens. Matter **23**, 053201 (2011).
[37]M. D. Segall, P. J. D. Lindan, M. J. Probert, C. J. Pickard, P. J. Hasnip, S. J. Clark, and M. C. Payne, "First-principles simulation: Ideas, illustrations and the CASTEP code," J. Phys.: Condens. Matter **14**, 2717 (2002).
[38]J. P. Perdew, K. Burke, and M. Ernzerhof, "Generalized gradient approximation made simple," Phys. Rev. Lett. **77**, 3865–3868 (1996).
[39]G. Kresse and J. Furthmüller, "Efficiency of ab-initio total energy calculations for metals and semiconductors using a plane-wave basis set," Comput. Mater. Sci. **6**, 15–50 (1996).
[40]G. J. Martyna, M. L. Klein, and M. E. Tuckerman, "Nosé–Hoover chains: The canonical ensemble via continuous dynamics," J. Chem. Phys. **97**, 2635–2643 (1992).
[41]K. Parlinski, Z. Q. Li, and Y. Kawazoe, "First-principles determination of the soft mode in cubic ZrO_2," Phys. Rev. Lett. **78**, 4063–4066 (1997).
[42]A. Togo, F. Oba, and I. Tanaka, "First-principles calculations of the ferroelastic transition between rutile-type and $CaCl_2$-type SiO_2 at high pressures," Phys. Rev. B **78**, 134106 (2008).
[43]P. Giannozzi, S. Baroni, N. Bonini, M. Calandra, R. Car, C. Cavazzoni, D. Ceresoli, G. L. Chiarotti, M. Cococcioni, I. Dabo, A. Dal Corso, S. de Gironcoli, S. Fabris, G. Fratesi, R. Gebauer, U. Gerstmann, C. Gougoussis, A. Kokalj, M. Lazzeri, L. Martin-Samos, N. Marzari, F. Mauri, R. Mazzarello, S. Paolini, A. Pasquarello, L. Paulatto, C. Sbraccia, S. Scandolo, G. Sclauzero, A. P. Seitsonen, A. Smogunov, P. Umari, and R. M. Wentzcovitch, "Quantum ESPRESSO: A modular and open-source software project for quantum simulations of materials," J. Phys.: Condens. Matter **21**, 395502 (2009).
[44]P. B. Allen and R. C. Dynes, "Transition temperature of strong-coupled superconductors reanalyzed," Phys. Rev. B **12**, 905–922 (1975).
[45]R. Hill, "The elastic behaviour of a crystalline aggregate," Proc. Phys. Soc., London, Sect. A **65**, 349–354 (1952).
[46]X.-Q. Chen, H. Niu, D. Li, and Y. Li, "Modeling hardness of polycrystalline materials and bulk metallic glasses," Intermetallics **19**, 1275–1281 (2011).
[47]A. R. Oganov, J. Chen, C. Gatti, Y. Ma, Y. Ma, C. W. Glass, Z. Liu, T. Yu, O. O. Kurakevych, and V. L. Solozhenko, "Ionic high-pressure form of elemental boron," Nature **457**, 863–867 (2009).
[48]Y. Chen, Q.-M. Hu, and R. Yang, "$P6_222$ phase of yttrium above 206 GPa from first principles," Phys. Rev. B **84**, 132101 (2011).
[49]Y. Wu, P. Lazic, G. Hautier, K. Persson, and G. Ceder, "First principles high throughput screening of oxynitrides for water-splitting photocatalysts," Energy Environ. Sci. **6**, 157–168 (2013).

[50]A. D. Becke and K. E. Edgecombe, "A simple measure of electron localization in atomic and molecular systems," J. Chem. Phys. **92**, 5397–5403 (1990).
[51]R. Dronskowski and P. E. Bloechl, "Crystal orbital Hamilton populations (COHP): Energy-resolved visualization of chemical bonding in solids based on density-functional calculations," J. Phys. Chem. **97**, 8617–8624 (1993).
[52]Z.-j. Wu, E.-j. Zhao, H.-p. Xiang, X.-f. Hao, X.-j. Liu, and J. Meng, "Crystal structures and elastic properties of superhard IrN_2 and IrN_3 from first principles," Phys. Rev. B **76**, 054115 (2007).